Oncogene (2002) 21, 4508–4520

www.nature.com/onc

Analysing c-kit internalization using a functional c-kit-EGFP chimera containing the fluorochrome within the extracellular domain

Thomas Jahn[1,3], Petra Seipel[1], Sunita Coutinho[1], Susanne Urschel[1], Kathleen Schwarz[1], Cornelius Miething[1], Hubert Serve[2], Christian Peschel[1] and Justus Duyster*[,1]

[1]*Department of Internal Medicine III, Laboratory of Leukemogenesis, Technical University of Munich, Germany;* [2]*Department of Internal Medicine A, University of Muenster, Germany*

In order to investigate activation and internalization of c-kit we created a functional c-kit-EGFP chimera by inserting EYFP (enhanced yellow fluorescent protein) within the extracellular domain of c-kit immediately downstream of the signal sequence, SS-EYFP-kit. This location was chosen because the C-terminal fusion of EGFP to c-kit unexpectedly caused constitutive activation of the c-kit tyrosine kinase. As analysed in fixed cells and by real time imaging *in vivo*, SCF induced activation led to internalization of the fusion construct and translocation to punctate structures resembling vesicles. Analysis of the internalization process by time lapse imaging revealed high mobility and discontinuous movement of these vesicles and their predominantly radial tracks. Two subsets of vesicles were observed: Traffic of the majority of vesicles was directed from the periphery to the center of the cell and most likely represents the internalization of activated receptor molecules via the endosomal pathway. However, some vesicular structures were observed to move towards the periphery of the cell and probably contain newly synthesized protein to replace internalized receptor molecules. The calculated velocity of moving vesicles ranged from 0.05 to 0.2 μm per se. Vesicle formation upon SCF induced dimerization of the receptor was strictly dependent on kinase activity of c-kit. Treatment of cells with phenylarsine oxide, an agent blocking receptor internalization, prior to SCF stimulation resulted in abrogation of the translocation of the chimera to vesicles whereas accumulation of vesicles was observed when cells were treated with proteasome inhibitors. Cholesterol depletion of the cell membrane by methyl-β-cyclodextrin resulted in dose dependent reduction of receptor internalization indicating that c-kit may be present in lipid rafts or that intact lipid rafts are required for efficient internalization of the receptor. Using the induction of vesicular structures as a sign of efficient internalization of the receptor analysis of mutant c-kit constructs deficient either in activation of PI3-Kinase or Src revealed that internalization of c-kit is dependent on recruitment of Src but not PI3-Kinase.
Oncogene (2002) **21,** 4508–4520. doi:10.1038/sj.onc.1205559

Keywords: c-kit; EGFP; signal transduction; PI3-kinase; Src

Introduction

The integrity of the c-kit signaling pathway is crucial for normal hematopoiesis, melanogenesis and gametogenesis (for a review see (Broudy, 1997)). Activation of this type III receptor tyrosine kinase (RTK) results from the binding of its ligand, stem cell factor (SCF, also known as kit ligand or steel factor), which exists in both soluble and membrane bound form (Langley *et al*., 1993; Longley *et al*., 1997). Activation of c-kit leads to autophosphorylation of the cytoplasmic tail encoding the tyrosine kinase and recruitment of a variety of signaling proteins to the receptor. In addition to the multitude of signaling pathways directly activated by c-kit (Blume-Jensen *et al*., 2000; Caruana *et al*., 1999; Deberry *et al*., 1997; Krystal *et al*., 1998; Serve *et al*., 1995; Thommes *et al*., 1999; Timokhina *et al*., 1998; Wakioka *et al*., 1999) there is evidence that the c-kit receptor also takes part in cytokine receptor cross talk in which type I receptors, e.g. the erythropoietin receptor, are activated by c-kit (Liu *et al*., 1994; Wu *et al*., 1995). In addition, c-kit can be activated by Bcr-Abl in absence of its ligand and might in turn function as a multiplier of foreign cytokines or oncogenes (Clarkson *et al*., 1997; Hallek *et al*., 1996). Subsequent to SCF induced activation of c-kit ubiquitination and clathrin-mediated internalization of activated c-kit molecules represent a negative feedback mechanism, which controls SCF mediated c-kit activation (Broudy *et al*., 1999; Miyazawa *et al*., 1994). It has been shown that after ligand induced downregulation of c-kit new protein production is necessary for reappearance of the c-kit receptor on the cell surface (Shimizu *et al*., 1996).

*Correspondence: J Duyster, Department of Internal Medicine III, Laboratory of Leukemogenesis, Technical University of Munich, Ismaningerstr. 22, 81675 Munich, Germany;
E-mail: justus.duyster@lrz.tum.de
[3]Current address: Childrens Hospital Los Angeles, Division of Research Immunology, IBMT, USC, 4650 Sunset Blvd., Los Angeles, CA 90027, USA; E-mail: TJahn@chla.usc.edu
Received 10 January 2002; revised 29 March 2002; accepted 4 April 2002

Fusion of EGFP to growth factor receptors has mainly been used to study receptor internalization following ligand-induced activation (Carter and Sorkin, 1998). The generation of different mutants of EGFP (EBFP, EYFP and ECFP) has tremendously enlarged the possibilities of *in vivo* studies of labeled proteins. Fluorescence resonance energy transfer (FRET) between two fluorochromes as a result of direct interaction of two labeled proteins has expanded the method of colocalization of two proteins (Gordon *et al*., 1998; Mahajan *et al*., 1998). A FRET based method in combination with labeled antibodies has been used to further elucidate the SCF induced dimerization process of c-kit molecules (Broudy *et al*., 1998). However, this procedure is crucially dependent on the use of well-characterized, non-activating and non-blocking antibodies, which recognize the extracellular domain of c-kit, and requires labeling of the cells prior to stimulation. The clear advantages of an EGFP fusion construct are the lack of any labeling procedure. In addition, the construct can be overexpressed and detected in nearly every setting chosen for analysis of subcellular localization, activation or colocalization studies. Disadvantages of the use of EGFP for labeling proteins are primarily the rather large size of EGFP and possible differences in the biology between the fusion and native proteins. Tagging proteins with EGFP always requires thorough controls in order to assess the wild-type like character of the tagged protein. The recommendation to avoid EGFP-tagging close to functional domains of proteins is difficult to follow since tagging of proteins with EGFP is almost exclusively carried out at the N- or C-terminus of proteins. N-terminal regions often contain crucial information for further processing of the protein and C-terminal regions in type III RTKs may contain regulatory domains or docking sites for proteins regulating half life time or enzymatic activity.

The goal of the present study was to create a c-kit EGFP fusion construct in order to visualize and further analyse activation and internalization of c-kit without antibody related labeling procedures. For type III RTKs, the C-terminal fusion of EGFP seemed the most plausible way to obtain a tagged construct. However, the C-terminal fusion unexpectedly led to constitutive activation of c-kit. In contrast, insertion of EYFP directly downstream of the signal sequence did not alter the tyrosine kinase activity and had no influence on SCF induced tyrosine kinase activity. By creating a functional c-kit EGFP fusion construct we have developed a valuable tool to investigate c-kit activation and internalization.

Results

Expression and analysis of different c-kit-EGFP fusion constructs

To create a biologically active c-kit-EGFP fusion construct we fused EGFP in frame to the C-terminus of the murine c-kit cDNA, kit-C-EGFP (Figure 1, upper panel, see Materials and methods for details). The linker region was represented by a glycine repeat, which should reduce steric hindrances and allow correct folding of EGFP and the c-kit C-terminus (Feng *et al*., 1999; Fischer *et al*., 1997). Western blot analysis of a c-kit immunoprecipitation using an antibody which recognized an epitope within the murine c-kit C-terminus revealed expression of precursor (lower band) and membrane bound form (upper band) of c-kit (Figure 2a, lower panel, lane 3). Both bands ran about 30 kD higher than the corresponding bands of c-kit WT (Figure 2a, lower panel, lane 2) or of the kinase defective c-kit mutant W42 (D790N) (Figure 2a, lower panel, lane 4) due to the increase of size by the fused EGFP. However, analysis of the tyrosine phosphorylation status of this construct revealed strong constitutive phosphorylation in the absence of SCF (Figure 2a, upper panel, lane 3 and Figure 2b, upper panel, lane 1) in contrast to c-kit WT showing only low level background phosphorylation or the W42 mutant of c-kit lacking detectable tyrosine phosphorylation (Figure 2a, upper panel, compare lanes 2, 3 and 4). Insertion of the silencing mutation W42 into the construct, kit-C-EGFP W42, abolished the constitutive phosphorylation (Figure 2b, upper panel, lane 2). Comparison and alignment of the phosphorylated band with the two forms (precursor and mature form) of kit-C-EGFP revealed that only the mature, membrane-bound form is constitutively activated and phosphorylated (Figure 2b). These observations suggest that C-terminal fusion of EGFP to the entire c-kit cytoplasmic tail selectively activates the membrane-bound form of c-kit.

To choose an inert location for the EGFP and to preserve a functional signal sequence, correct processing, normal glycosylation and membrane localization of a c-kit EGFP chimera we decided to fuse the fluorochrome immediately downstream of the signal sequence with murine c-kit (SS-EYFP-kit, Figure 1, second panel). To facilitate detection of c-kit in future co-localization studies EYFP was inserted instead of EGFP. EYFP is an EGFP mutant differing from EGFP in excitation and emission characteristica. EYFP was equipped with N- and C-terminal glycine linkers to reduce conformational disturbances (Figure 1, lower panel). SS-EYFP-kit overexpressed in COS7 cells (Figure 2c, lower panel, lanes 1 and 2) was not constitutively activated in absence of SCF and became strongly phosphorylated upon addition of SCF (Figure 2c, upper panel, lanes 1 and 2) which indicates that SCF binding to the extracellular portion of c-kit was not perturbed by the 27 kD sized fluorochrome. Only the membrane bound mature form became tyrosine phosphorylated and precursor and membrane bound were present (Figure 2d, upper and lower panels). To verify the biological activity of the chimera, we analysed Aht activation (Figure 2e) and the ability of the constitutively activating mutation D814V to induce IL-3 independent growth of Ba/F3 cells. As shown in Figure 2f Ba/F3 cells expressing cKit D814V or SS-

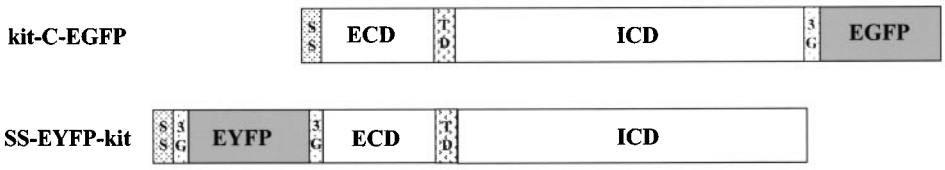

Figure 1 kit-EGFP fusion constructs – kit-C-EGFP; EGFP was fused in frame to the C-terminus of the murine c-kit cDNA. A linker of three glycines (3G) was inserted between c-kit and EGFP in order to reduce steric hindrances and allow correct folding. SS-EYFP-kit: An *Eco*RI site immediately after the signal sequence of c-kit was inserted by PCR based site directed mutagenesis and used for insertion of EYFP. EYFP was framed with glycine repeats. SS (signal sequence); ECD (extracellular domain); TD (transmembrane domain)

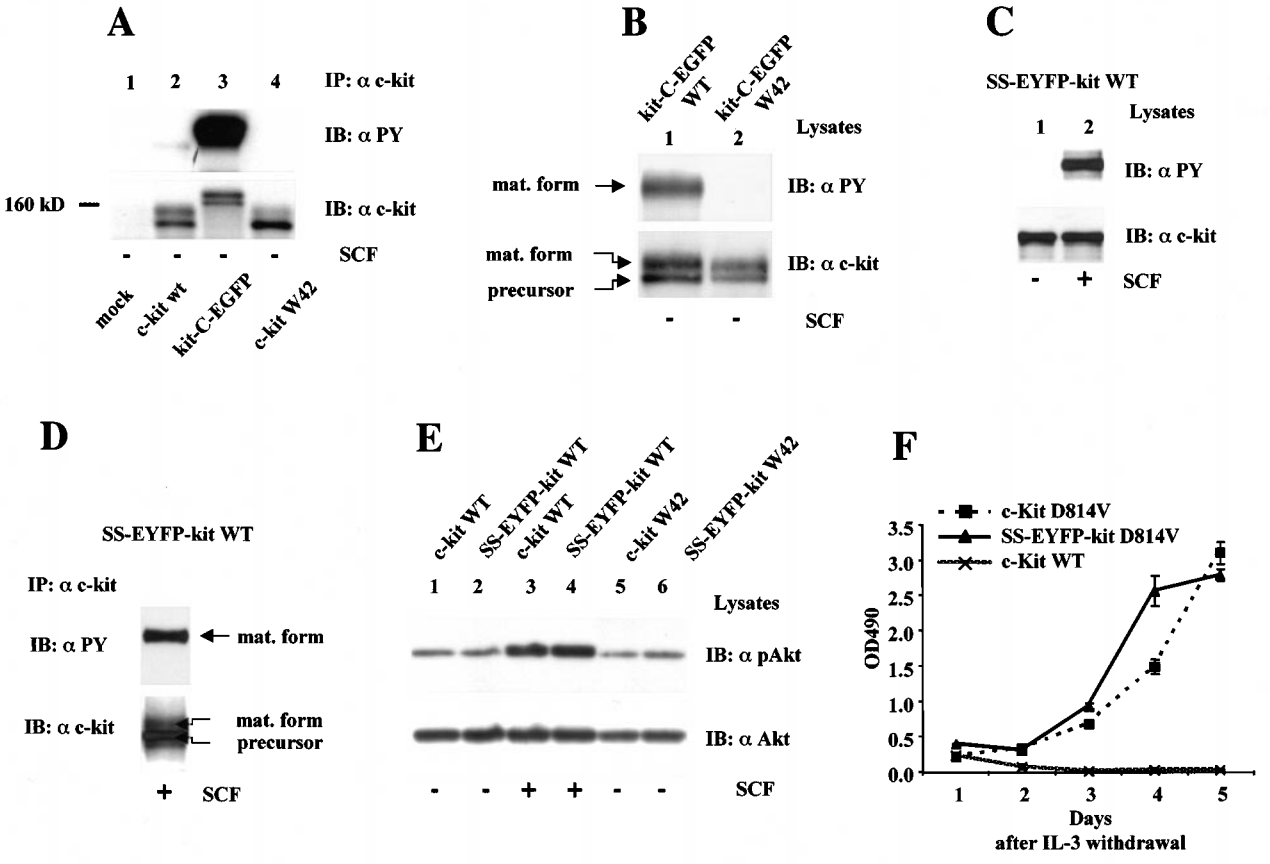

Figure 2 (**a**) c-kit-C-EGFP is constitutively activated: A c-kit immunoprecipitation from 293 cells transiently expressing empty vector (mock, lane 1), WT c-kit, kit-C-EGFP, c-kit W42 (kinase defective) was performed and bound fractions were resolved in SDS–PAGE. Western blot analysis was done first using an anti-phosphotyrosine antibody (upper panel) and after stripping of the blot with an anti c-kit antibody (lower panel). (**b**) Only the mature form of kit-C-EGFP is constitutively tyrosine phosphorylated. Lysates from COS1 cells transiently expressing kit-C-EGFP WT or kit-C-EGFP W42 were separated on SDS–PAGE and analysed with an anti-phosphotyrosine (upper panel) and with an anti-kit antibody (lower panel) (**c**) SS-EYFP-kit WT shows regular SCF induced autophosphorylation. SS-EYFP-kit was expressed in COS7 cells and lysates from unstimulated (lane 1) and SCF stimulated cells (lane 2) were run on SDS–PAGE and tested for SCF induced phosphorylation (upper panel) and expression of the construct (lower panel). (**d**) SS-EYFP-kit is correctly processed from precursor to mature membrane bound form. An immunoprecipitation from COS7 cells expressing SS-EYFP-kit WT was run on SDS–PAGE and Western blot analysis with anti-phosphotyrosine antibody (upper panel) and anti-c-kit antibody (lower panel) was performed. Precursor and membrane bound form of SS-EYFP-kit are indicated by an arrow. Exact alignment of the bands revealed phosphorylation of the membrane bound form of the construct. (**e**) Stimulation of SS-EYFP-kit WT results in activation of PKB/Akt. COS7 cells were co-transfected with HA-tagged PKB/Akt and equal amounts of DNA of the different c-kit constructs cloned in the same vector background (pCDNA 3.1): c-kit WT or SS-EYFP-kit WT or the corresponding W42 mutants of these constructs. SCF stimulation results in comparable PKB/Akt activation as analysed by probing lysates with an anti-phospho-Akt antibody (upper panel). Equal amounts of the HA-tagged Akt construct were expressed in unstimulated and stimulated cells (lower panel). (**f**) Growth factor independent proliferation of Ba/F3 cells stably expressing c-kit, D814 V or SS-EYFP-kit D814V: Cells were plated into 96-well plates at the density of 3×10^4 cells per well. After the indicated time period, the viable cells in each well were assayed to test their ability to transform MTS into a purple formazan. The absorbance of the samples was measured in an ELISA reader at 490 nm

EYFP-Kit D814V showed comparable IL-3 independent proliferation. Ba/F3 cells stably expressing c-kit WT failed to survive or proliferate in media lacking IL-3.

SCF induced internalization of SS-EYFP-kit

Having confirmed that SS-EYFP-kit exhibits correct processing and becomes regularly activated by SCF we were interested in directly imaging the changes in the subcellular distribution pattern of c-kit upon stimulation with SCF. SCF-induced activation of c-kit has been reported to lead to internalization and subsequent degradation of the receptor via the ubiquitin/endosomal pathway. In nonstimulated cells expressing SS-EYFP-kit there was a diffuse to patch like fluorescence signal from the whole cell which is compatible with membrane localization (Figure 3a). Protein production from this construct was evidenced by a bright fluorescence signal from the ER. Imaging of the cells 20 min after addition of SCF revealed the formation of dot like structures distributed over the whole cell (Figure 3b). Z-scan analysis localized these dots to the membrane or to the cytoplasm close to the membrane (Figure 3c and d). These dots resembled vesicles and represented most likely early endosomes containing internalized c-kit molecules.

Time lapse imaging of SCF-induced internalization of SS-EYFP-kit molecules

When living cells expressing SS-EYFP-kit were observed after stimulation with SCF, rapid movement and fluctuation in size and intensity of these vesicles was observed. This observation excluded that formation of the punctate structures was artificially induced by the fixation method previously used. We performed time lapse imaging of living cells to determine direction and velocity of these vesicles. COS7 cells transiently expressing SS-EYFP-kit were stimulated with SCF and cells showing vesicle formation were observed for 200 s. Figure 4a shows a cell, which was observed for 200 s at an imaging cycle time of 10 s. The cellular projection of the summary of all vesicle tracks during 200 s revealed a mainly radial pattern (Figure 4b). Movement of these vesicles mostly appeared to be directed from the periphery to the perinuclear region of the cell (Figure 4c) but the movement in the opposite direction was also observed (Figure 4d). Subsequent vesicles from the same area of the cell moved on the same track revealing guided movement most likely along filamentous structures. Similar observations were made in other cells. Interestingly, movement of the vesicles seemed to be rather non-continuous, since the distances between to subsequent locations vary considerably (in panel c compare distance between t_1/t_2 and t_2/t_3, time difference is 10 s). The calculated velocity of this vesicle ranged from 0.05 μm/s (between t_1/t_2) to 0.2 μm/s (between t_2/t_3).

The observation of vesicles moving in opposite directions upon stimulation suggested that SCF induced internalization of the receptor was followed by rapid reconstitution of membrane bound c-kit by newly synthesized protein or by recycling of previously internalized receptor molecules. In order to determine if the c-kit receptor undergoes recycling or if new protein synthesis is necessary for reappearance of c-kit at the cell surface we analysed the kinetics of receptor constitution after SCF stimulation with and without treatment of the cells with cycloheximide (Figure 4e). Reconstitution of c-kit on the surface of Ba/F3 cells stably expressing c-kit following SCF stimulation is inhibited in cells treated with cycloheximide. Complete reconstitution of c-kit on the cell surface was observed 90 min after SCF stimulation under the conditions of the c-kit cDNA driven by a constitutively active CMV promoter whereas cells incubated with cycloheximide failed to show significant reconstitution of c-kit (Figure 4e, compare lower left and right panel). Our data are consistent with results from Shimizu *et al*. (1996) showing that new protein and RNA synthesis are required for reappearance of c-kit after SCF stimulation. In line with these results, the half-life time of c-kit WT was significantly decreased upon stimulation of the receptor with SCF (Figure 4f, compare upper and lower panel). Taken together these results are compatible with the hypothesis that vesicles on their way from the cell periphery to the center contain internalized c-kit receptor whereas the vesicles moving in the opposite direction deliver newly synthesized c-kit molecules to the cell membrane.

Role of c-kit tyrosine kinase activity

For native c-kit it has been shown that inactivation of the kinase domain resulted in a reduced rate of internalization of ligand-receptor complexes (Yee *et al*., 1994). In order to determine the influence of the kinase activity on vesicle movements two mutants were created: Introduction of the W42 (D790N) mutation into the chimera resulted in the expected loss of inducible tyrosine kinase activity upon binding of SCF (Figure 5a, upper panel, lanes 3 and 4) (Li *et al*., 1996). An activating mutation (V558G) of c-kit was introduced into the chimera and constitutively activated the fusion construct as anticipated (Figure 5a, upper panel, lanes 5 and 6) (Kanakura *et al*., 1994).

We compared the localization pattern of SS-EYFP-kit WT, the W42 mutant lacking inducible tyrosine kinase activity, and the constitutively active mutant of c-kit, V558G with or without SCF stimulation (Figure 5). Cells were fixed 20 min after addition of SCF and most cells expressing SS-EYFP-kit WT showed vesicle formation (Figure 5b and c). In contrast, no vesicle formation was observed in cells expressing the kinase defective mutant W42 (Figure 5d and e). Addition of SCF to cells expressing the constitutively active mutant of c-kit V558G did not alter the localization pattern (Figure 5f and g). In some cells constitutive vesicle formation was observed possibly reflecting constitutive internalization since exchange of Valine to Glycine at position 558 causes constitutive dimerization and activation of c-kit independent of ligand induced dimerization.

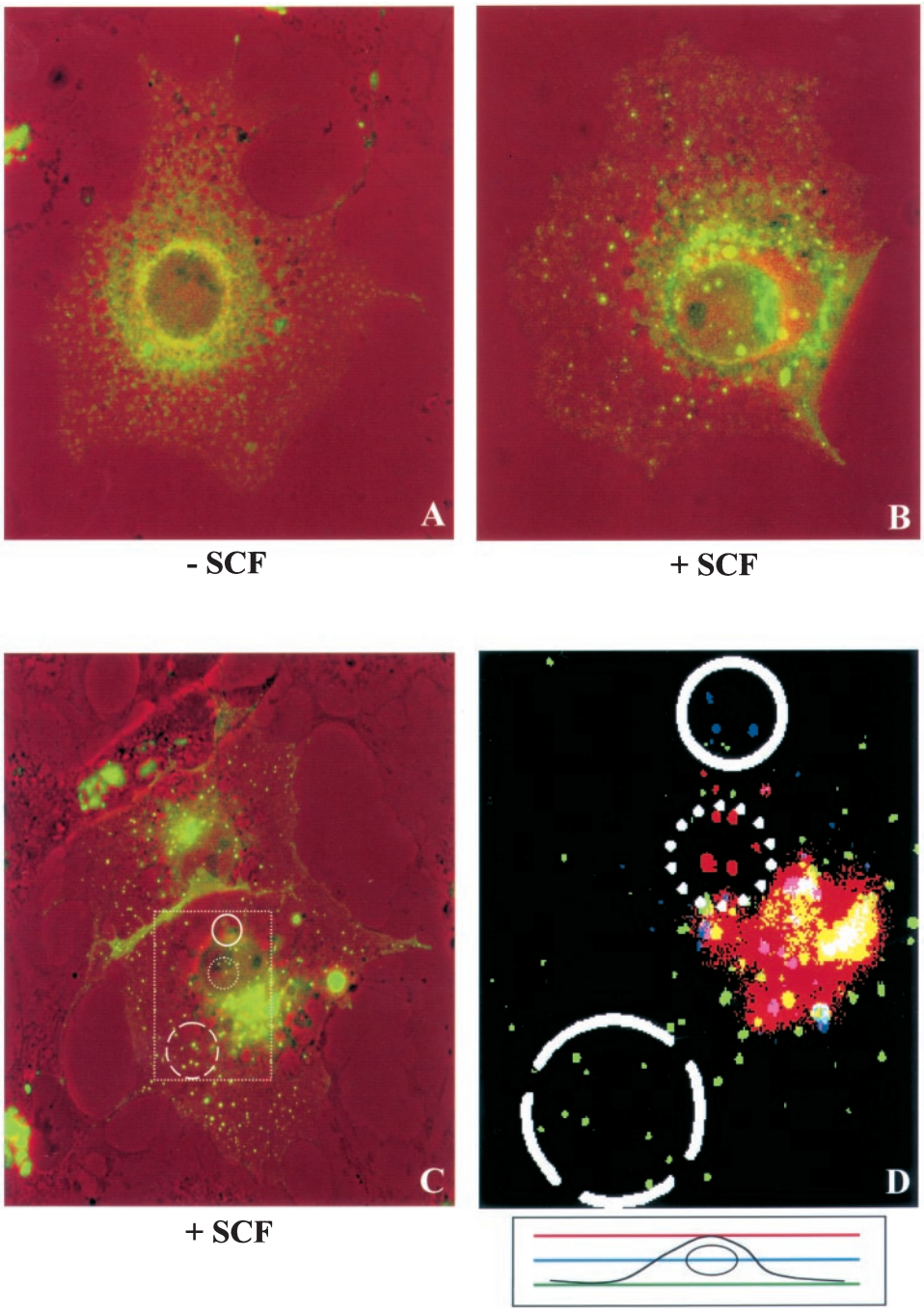

Figure 3 SCF induced internalization of SS-EYFP-kit–COS 7 cells transiently expressing the fusion constructs as indicated were cultured on chamber slides, serum starved for at least 6 h and unstimulated (-SCF) or stimulated with SCF (+SCF). The fluorescence information of the c-kit-fusion constructs (green channel) is superimposed on the transmission picture of the cell (red channel) in order to facilitate subcellular localization of the fluorescence signal (**a**–**c**). A Z-Scan analysis was performed with a cell showing internalization of c-kit (**c** and **d**), see Materials and methods for details. (**d**) Shows an enlargement of the cell from (**c**) and the overlay picture contains the fluorescence information of three layers of the same area. The three circles circumvent punctate structures focused at the highest level over the nucleus (red dots, punctate line), the epinuclear layer of the cell (blue dots, closed line) and the lower level of the periphery of the cell (green dots, interrupted line). The three channels were combined to one RGB image (**d**)

Role of tyrosine 719 and tyrosines 567/569 for the internalization of activated c-kit

Activation of PI3-Kinase has been reported to be a crucial step in finally directing the internalized PDGF receptor to the degradative pathway following receptor activation (Joly *et al*., 1995). Phosphotyrosine 719 (Y719) is the binding site of the C-terminal SH2 domain of the p85 subunit of PI3-kinase. Integrity of this site is a prerequisite for c-kit induced PI3-kinase

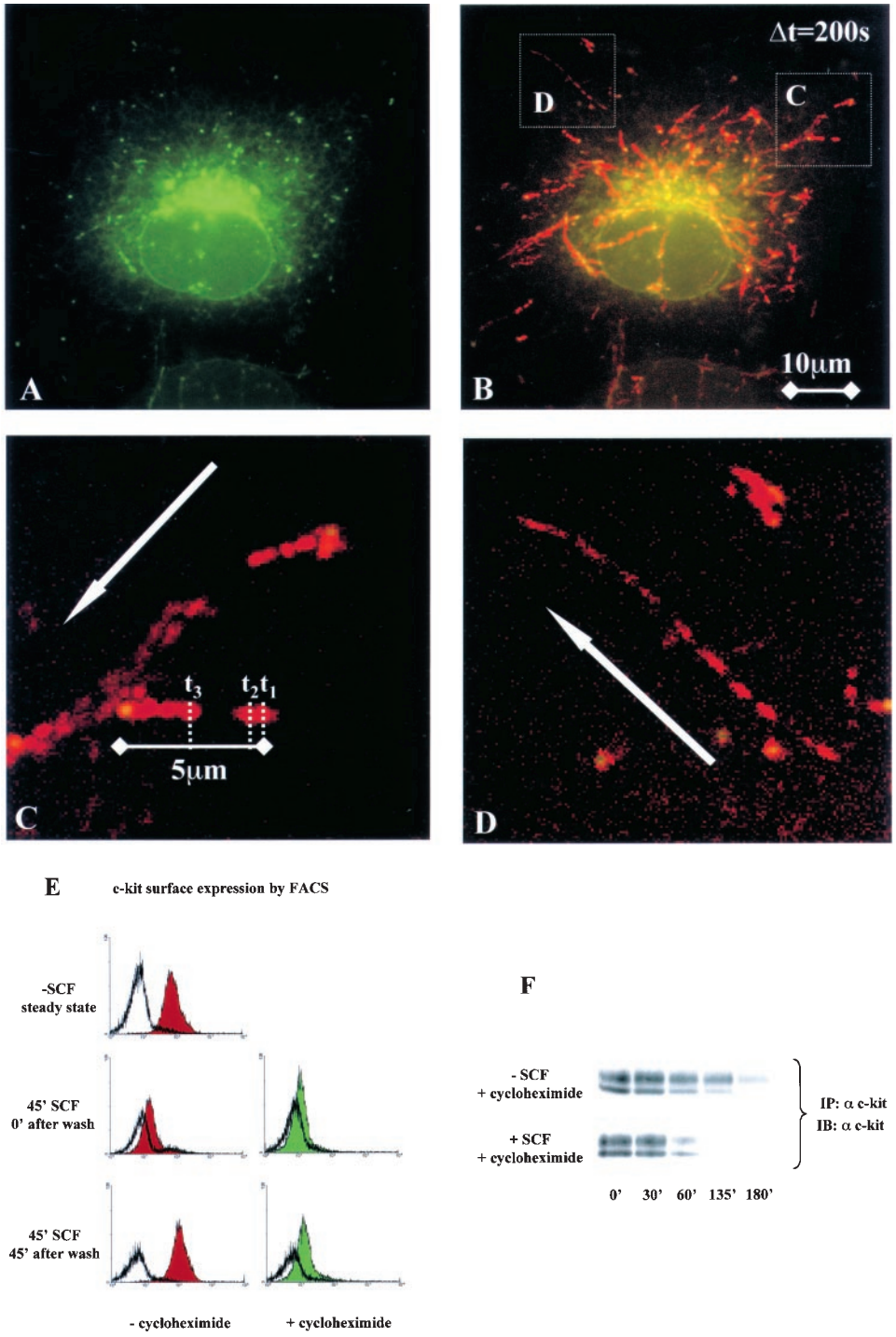

Figure 4 Time lapse imaging of SCF induced internalization of SS-EYFP-kit molecules in living cells – COS7 cells expressing SS-EYFP-kit WT were grown on a dish with integrated coverslide. Time lapse imaging of a cell showing SCF induced vesicle formation (**a**, initial picture) was performed at 37°C for 200 s with an imaging cycle time of 10 s. The sum of all vesicle movements during 200 s ($\Delta t = 200$ s) (red channel) was superimposed onto the initial picture of the cell (green channel) (**b**) Vesicle tracks were mostly radially arranged. Directions to the center of the cell as well as to the periphery were observed (**c** and **d**, zoomed from **b**). Reconstitution of the c-kit receptor following SCF induced downregulation: Ba/F3 cells stably expressing cKit WT were analysed for surface cKit expression before and after 45′ treatment with 500 ng/ml SCF with or without addition of 75 μg/ml (267 μM) cycloheximide (**e**). To assess reconstitution of c-kit at the cell surface, SCF containing media was removed, cells were washed three times with PBS and cultivated for the indicated additional time with or without cycloheximide. For detection of c-kit expression by FACS, cells were stained with a PE-labeled anti c-kit antibody ACK45, or control antibody, A95-1, and measured using FACS in the FL1 and FL2 gate. (**f**) Influence of SCF stimulation on the half life time of c-kit: SCF stimulated and non-stimulated COS1 cells overexpressing c-kit WT were treated with 100 μg/ml (355 μM) cycloheximide and bound fractions of c-kit immunoprecipitations were analysed with an anti c-kit antibody at the indicated times

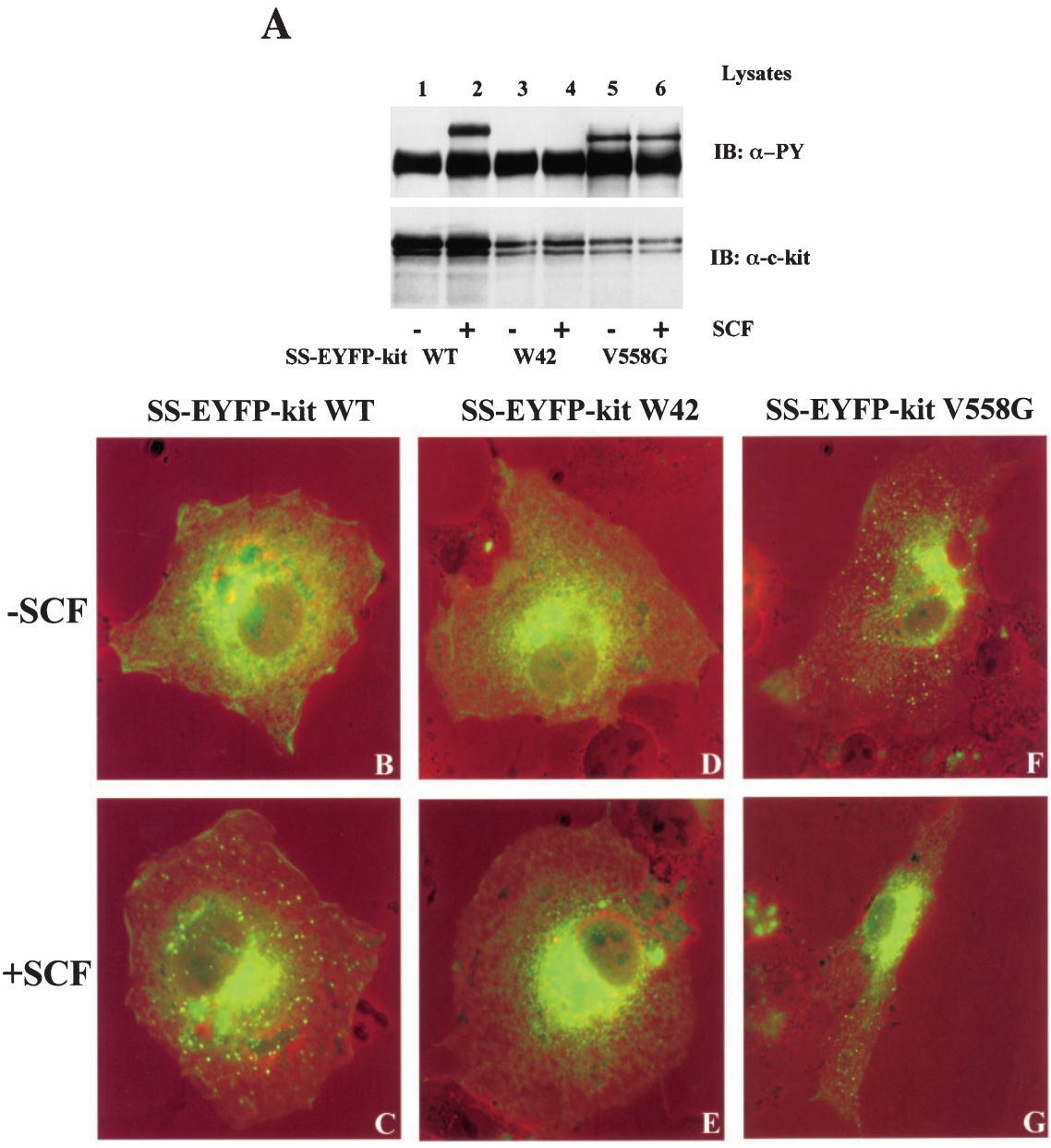

Figure 5 Internalization of SS-EYFP-kit requires tyrosine kinase activity – (**a**) Lysates of unstimulated and SCF treated COS7 cells transiently expressing SS-EYFP-kit WT (lanes 1/2), the kinase defective mutant W42 (D790N) (lanes 3/4) or the constitutively activated mutant V558G (lanes 5/6) were separated on SDS–PAGE and phosphorylation (upper panel) and expression of the SS-EYFP-kit constructs (lower panel) was examined by Western blot analysis. (**b**–**g**) COS7 cells expressing SS-EYFP-kit (**b**/**c**), the kinase defective W42 mutant (**d**/**e**) and the constitutively active mutant V558G (**f**/**g**) were plated on chamber slides and vesicle formation was compared between cells with and without SCF stimulation. The fluorescence information of the kit-fusion constructs (green channel) is superimposed on the transmission picture of the cell (red channel) in order to facilitate subcellular localization of the fluorescence signal

activity resulting in PKB/Akt activation. Accordingly, a tyrosine to phenylalanine mutant of Y719 (SS-EYFP-kit Y719F) failed to induce phosphorylation of co-expressed HA-tagged Akt (Figure 6a, upper panel, compare lanes 1 and 2). Tyrosines 567 and 569 have been reported to be involved in Src activation. To verify the biological activity of SS-EYFP-kit YY567/569FF we compared its capacity to activate Akt and it was found to be equal to SS-EYFP-kit WT (Figure 6b). In order to define the role of PI3-Kinase and Src in the internalization process of SCF activated c-kit we wished to analyse SCF induced internalization of these constructs. Mutation of the PI3-Kinase binding site (Y719) did not influence c-kit internalization as analysed by vesicle formation upon SCF stimulation (Figure 6e and f, compare with SS-EYFP-kit WT, Figure 6c and d), whereas mutation of tyrosines

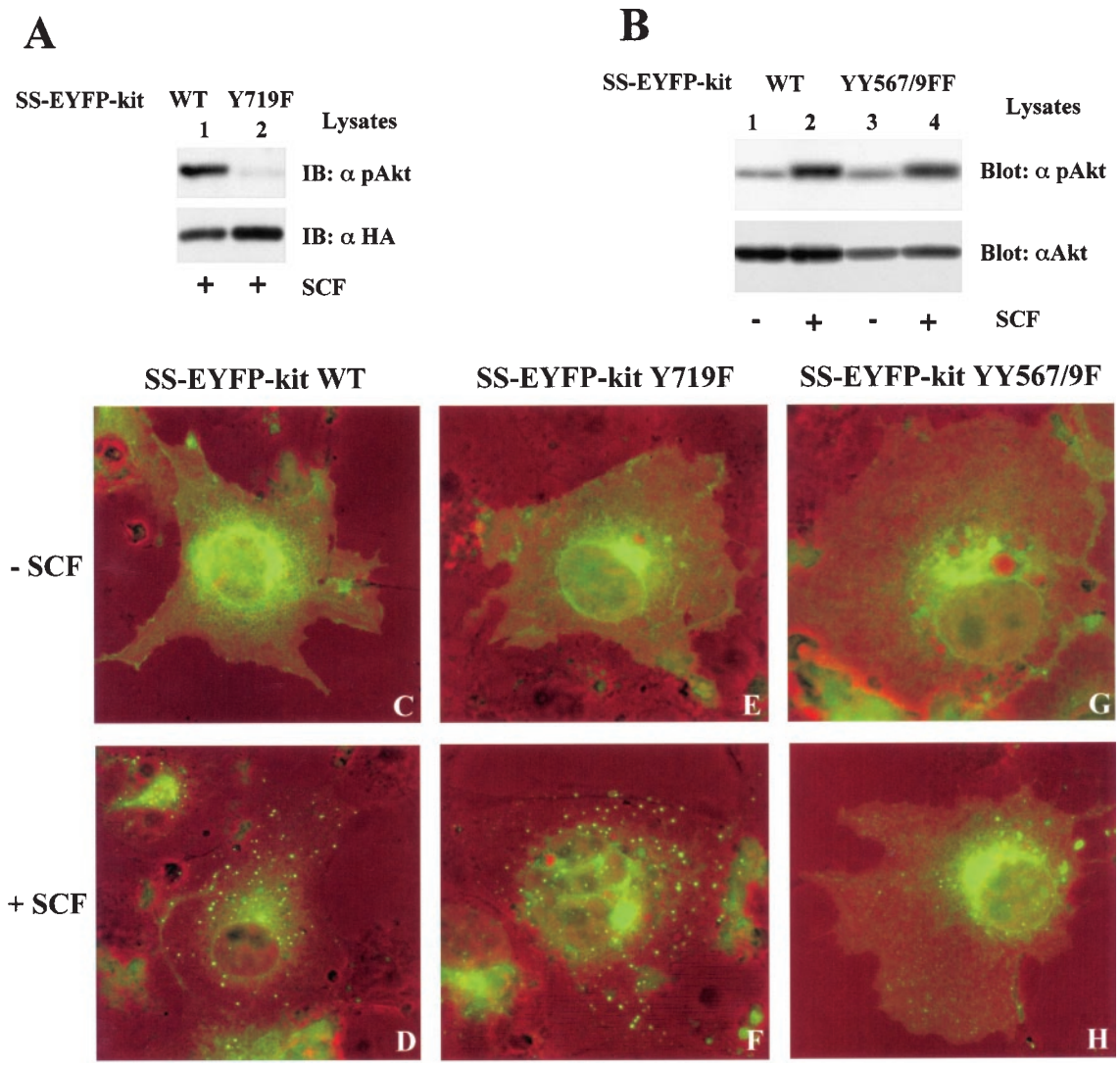

Figure 6 Role of tyrosine 719 and tyrosines 567/569 in internalization of activated c-kit: (**a**) Lysates from SCF stimulated COS7 cells co-expressing HA-Akt and SS-EYFP-kit WT (lane 1) or the Y719F mutant (lane 2) were analysed for activation of PKB/Akt by Western blotting with a phosphospecific anti-pAkt antibody (upper panel). Similar amounts of HA-Akt were expressed (lower panel). (**b**) Lysates from cells expressing HA Akt, SS-EYFP-kit WT or YY567/569FF were analysed for Akt activation following SCF stimulation using a phospho-specific Akt antibody (upper panel). Akt levels were roughly equal (lower panel). (**c**–**h**) COS7 cells expressing SS-EYFP-kit WT (**c**/**d**), the Y719F mutant defective in PI3-kinase activation (**e**/**f**), and the mutant YY567/569FF (**g**/**h**) were plated on chamber slides and vesicle formation was compared between cells with and without SCF stimulation. The fluorescence information of the kit-fusion constructs (green channel) is superimposed on the transmission picture of the cell (red channel)

567 and 569 resulted in a significant decrease of visible dot like structures (Figure 6g and h).

Blocking of c-kit internalization by phenylarsine oxide (PAO) and accumulation of early endosomes by inhibition of proteasomes

In order to further define the vesicular structures containing SS-EYFP-kit after SCF induced activation we exposed the cells to two chemical agents interfering with receptor internalization and degradation at different levels: On the plasma membrane PAO forms ring structures with vicinal sulfhydryl groups and inhibits receptor internalization (Beaumont *et al*., 1998). Proteasome inhibitors like lactacystin block the proteasomal degradation as a late step of internalization. Cells expressing SS-EYFP-kit WT were preincubated with PAO for 5 min at 50 M, washed and then stimulated with SCF. In cells incubated in DMSO alone, translocation of SS-EYFP-kit to vesicles was clearly visible (Figure 7a), whereas in cells preincubated in PAO it was abrogated (Figure 7b). When cells were incubated for 15 min with proteasome inhibitors (Lactacystin, MG132, Proteasome Inhibitor I, 10 mM), washed, and then stimulated with SCF, vesicles containing internalized c-kit molecules showed an increase in size and number in most of the cells examined (Figure 7c). The observed vesicles therefore most likely represent early

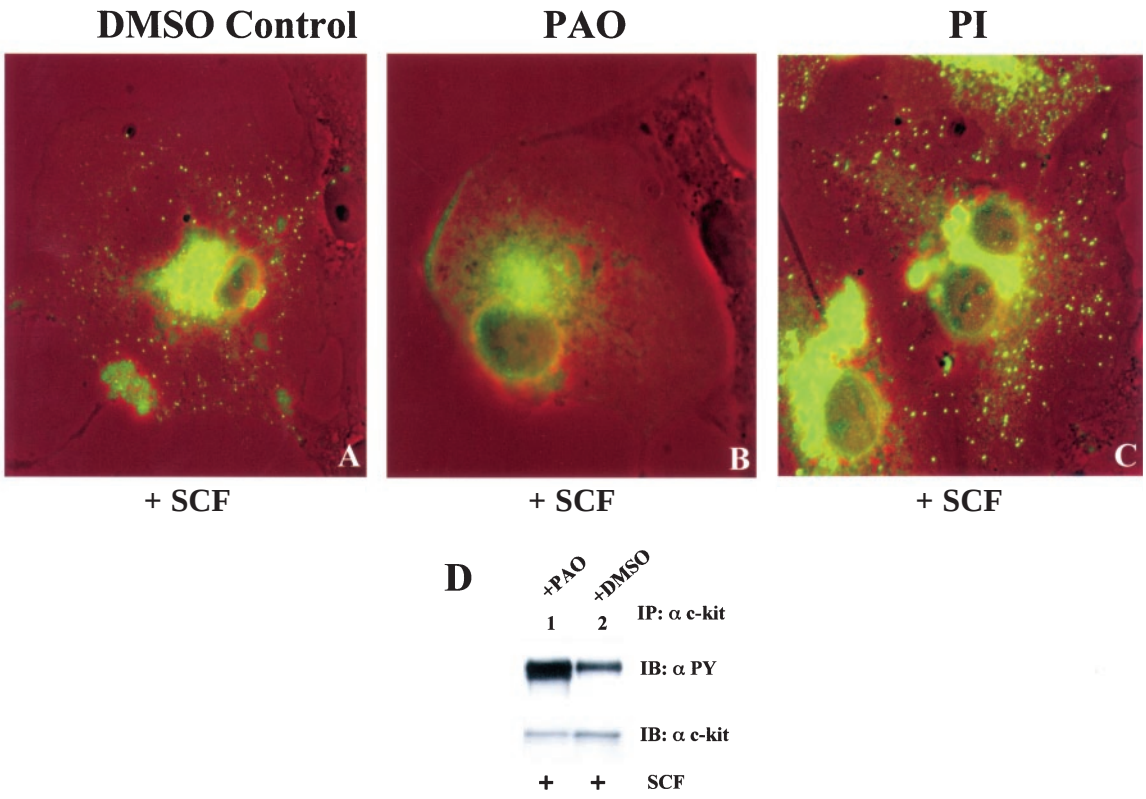

Figure 7 Treatment of the cells with phenylarsine oxide (PAO) abolished vesicle formation and inhibition of proteasomes led to accumulation of internalized c-kit. SS-EYFP-kit WT expressing cells were treated with DMSO (**a**), PAO (50 μM) (**b**) or cell permeable proteasome inhibitors (lactacystin, MG132, Proteasome Inhibitor I, 10 μM each) (**c**) for 5 min prior to stimulation with SCF. After 20 min of stimulation cells were fixed and examined for vesicle appearance. (**d**) A c-kit immunoprecipitation was performed from SCF stimulated COS1 cells expressing SS-EYFP-kit and treated with the same concentration of PAO (lane 1) and DMSO (lane 2) Bound fractions were analysed for phosphorylation (upper level) and amount of c-kit (lower level)

endosomes containing internalized SS-EYFP-kit molecules which are about to be degraded by the proteasome machinery of the cell. As a control we assessed tyrosine phosphorylation of SS-EYFP-kit from SCF stimulated cells treated with PAO to exclude that PAO influenced ligand induced phosphorylation of the receptor (Figure 7d). Upon PAO treatment of SCF induced phosphorylation was even enhanced possibly reflecting accumulation of phosphorylated receptor due to blocked internalization.

Cholesterol extraction from the cell membrane with methyl-β-cyclodextrin (MCD)

Cholesterol is an essential structural component of lipid raft membrane microdomains (Simons and Ikonen, 1997). To test whether c-kit function and internalization depends on the integrity of lipid rafts we analysed SCF-induced translocation of SS-EYFP-kit molecules in cells preincubated at different concentrations of MCD, a compound which has been shown to lead to the disruption of lipid rafts (Keller and Simons, 1998). Vesicle appearance was drastically reduced in cells incubated in 20 mM MCD for 45 min prior to stimulation (compare Figure 8a and b) and was completely abrogated in cells preincubated with 30 mM MCD (Figure 8c). This suggests that c-kit molecules could be present in lipid rafts and that these microdomains may be required for regular SCF-induced internalization of the receptor. Reduced internalization of the receptor is not due to diminished phosphorylation of the receptor since we observed even enhanced tyrosine phosphorylation of the receptor upon treatment of the cells with MCD (Figure 8d).

Discussion

The use of EGFP to visualize proteins has opened a wide field of applications including *in vivo* subcellular trafficking/colocalization studies and methods using the biochemical properties of EGFP, e.g. fluorescence resonance energy transfer (FRET) (Gordon *et al*., 1998), fluorescence recovery after photobleaching (FRAP) (Oliferenko *et al*., 1999), proximity imaging (PRIM) (De Angelis *et al*., 1998). With the EGF-receptor (epidermal-growth factor) C-terminal fusion of EGFP resulted in a construct unperturbed by the fusion with EGFP. This construct was successfully used to elucidate the internalization process of an RTK (Carter and Sorkin, 1998). The dimerization process of c-kit upon SCF stimulation has been analysed in a

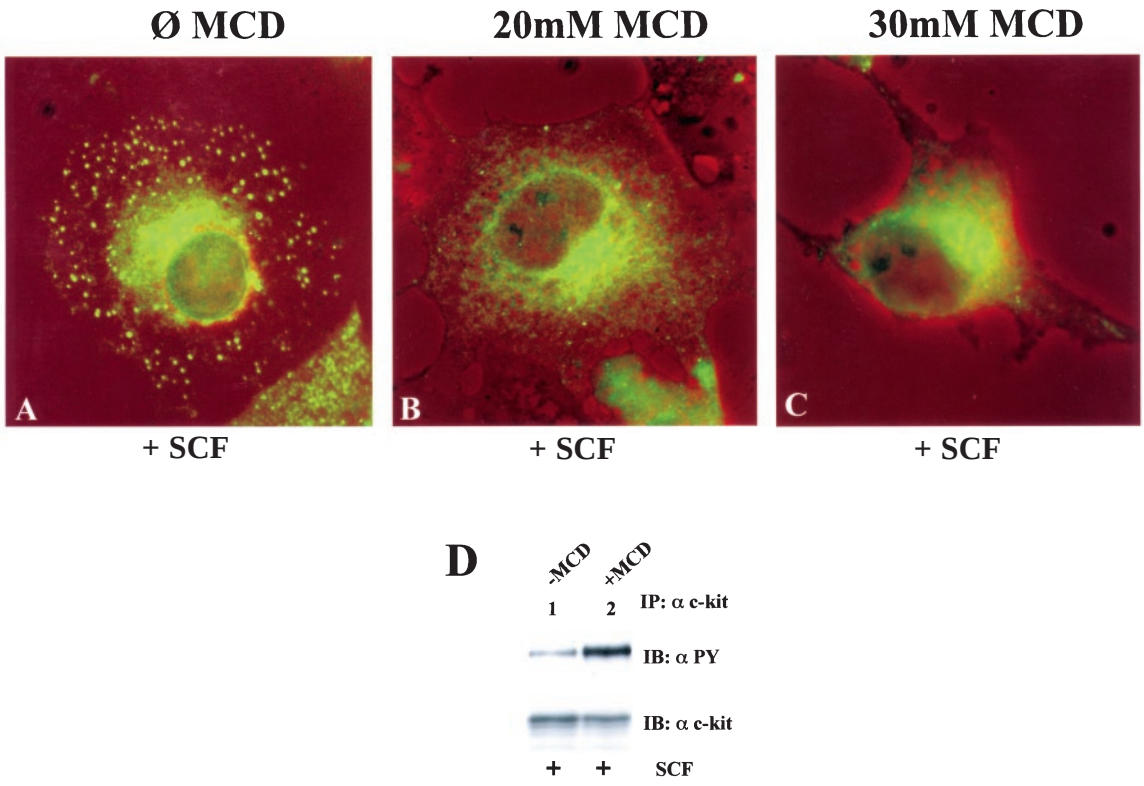

Figure 8 Preincubation of the cells with methyl-β-cyclodextrin inhibits internalization of c-kit–SS-EYFP-kit WT expressing cells were treated with MCD for 45 min prior to SCF stimulation. After 20 min of stimulation cells were fixed and examined for vesicle appearance. (**a**) Shows the control without MCD incubation and (**b**) and (**c**) show representative cells preincubated at 20 and 30 mM MCD, respectively. (**d**) A c-kit immunoprecipitation was performed from SCF stimulated COS1 cells expressing SS-EYFP-kit WT and treated with the 20 mM MCD (lane 2) and control media (lane 1) Bound fractions were analysed for phosphorylation (upper level) and amount of c-kit (lower level)

study using FRET in combination with fluorochrome labeled antibodies (Broudy *et al*., 1998).

In order to study the activation dependent internalization process of c-kit we were interested in the creation of a biologically active EGFP fusion construct which would overcome the need for the labeling procedure and would allow detection of c-kit in a broad range of analytical setting. Insertion of EYFP downstream of the signal sequence of c-kit created a functional fusion construct (SS-EYFP-*kit*) which showed comparable activity to c-kit WT as assessed by SCF induced tyrosine autophosphorylation and activation of PKB/Akt. Furthermore, expression of a constitutively activated mutant of SS-EYFP-kit in Ba/F3 cells led to the same extent of IL-3 independent growth compared to the non-tagged c-kit mutant. The unusual location of EYFP between signal sequence and extracellular domain was chosen because the simple C-terminal fusion unexpectedly caused constitutive activation of c-kit. The reason for this ligand-independent activation is unclear. Other receptors like the EGFR have been fused to EGFP in a similar way and apparently no constitutive activation has been observed (Carter and Sorkin, 1998). It is possible that the presence of EGFP at the C-terminus influences the folding of the kinase domain and hereby causes intramolecular activation. Interestingly, only the mature, fully processed form of this chimera exhibited constitutive tyrosine phosphorylation indicating that either glycosylation or localization to the membrane induces autophosphorylation of this c-kit-EGFP chimera. Our novel approach to create an extracellular fusion with EGFP might represent a general means to create an EGFP-receptor fusion protein, when the intracellular function is critically altered by EGFP.

We show that SCF induced activation of SS-EYFP-kit results in translocation of the fusion construct to endosomal vesicles. Vesicles were localized closed to the membrane as determined by Z-scan analysis and showed tremendous mobility as analysed by time lapse imaging. The observed tracks on which the vesicles moved were mostly radial and the directions of vesicles were mainly towards the perinuclear region and contain internalized receptor. However, vesicular structures moving towards the periphery were also observed. Since the c-kit receptor does not seem to become recycled, vesicles moving to the periphery of the cell most likely contain newly synthesized protein, which is transported to the surface. This hypothesis is in line with the kinetics of cycloheximide sensitive reconstitution of c-kit at the cell surface of Ba/F3 cells stably expressing c-kit. Interestingly, vesicle tracks

seemed to be rather non-variable and vesicles subsequently moving in the same or different directions in the same area of the cell were observed to use the same track. Therefore it might be speculated that these vesicles are transported along filaments.

We observed cells for 200 s with a cycle time of 10 s. Digital imaging of the vesicle tracks enables determination of the velocity of single vesicles and ranged from 0.05 to 0.2 μm/s. Since the distances between two subsequent locations of the same vesicle vary considerably, the vesicle movement seems to be rather non-continuous. This suggests that the machinery moving these vesicles seems to function in a 'stop-and-go' manner rather than in continuous and steady motion.

Internalization and appearance of c-kit in early endosomes required tyrosine kinase activity and was well detectable after about 20 min of SCF stimulation. Significantly, addition of SCF to cells expressing the W42 mutant fusion construct lacking inducible kinase activity did not result in visible vesicle formation. This result is in line with the observation that SCF stimulation of the W42 mutant led to internalization at a reduced rate (Yee *et al*., 1994). We hypothesized that constitutive activation of c-kit by dimerization of the V558G mutation might result in permanent internalization of c-kit molecules and subsequent constitutive vesicle formation. Constitutive vesicle formation was seen in some cells expressing SS-EYFP-kit V558G, but not in all, and no change was apparent after addition of SCF. In line with this observation, Western blot analysis did not show enhanced tyrosine phosphorylation of SS-EYFP-kit V558G after stimulation with SCF.

The mutant Y719F deficient in the activation of the PI3-kinase pathway showed similar vesicle formation upon ligand induced activation of the receptor. This observation is in line with a previous report stating similar internalization of c-kit WT and the Y719F mutant under normal conditions (Gommerman *et al*., 1997). For the PDGF receptor Joly *et al*. (1995) have reported that PI3-kinase binding sites are not required for internalization of PDGF receptor but are required to divert the PDGF receptor to a degradative pathway. In contrast, for the Flt3/Flk2 receptor tyrosine kinase Beslu *et al*. (1996) have shown that PI3-Kinase is not required for mitogenesis or internalization of the receptor. It seems that the internalization process itself does not depend on activation of PI3-Kinase, whereas the further degradation of the mentioned receptors seems to be differentially affected by this pathway. Interestingly, SCF induced translocation of mutants Y567F and 569 (both sites have been reported to be involved in SCF induced Src activation (Lennartson *et al*., 1999)) to vesicular structures was significantly reduced. Consistent with this finding, pharmacological inhibition of Src has been shown to result in abolishment of c-kit internalization upon stimulation with SCF (Broudy *et al*., 1999).

Vesicle appearance upon SCF stimulation of cells expressing SS-EYFP-kit WT was inhibited by phenylarsine, a trivalent arsenic which has been reported to interfere with receptor internalization by interaction with vicinal dithiols. In turn, vesicle accumulation was observed when proteasomes were blocked by addition of cell permeable proteasome inhibitors. Both observations taken together strongly suggest that the observed vesicles in fact represent structures of the endosomal pathway.

As a new aspect of receptor mediated signaling the involvement of lipid rafts as platforms for attachment of proteins has been proposed (Kurzchalia and Parton, 1999; Simons and Ikonen, 1997). Cholesterol-sphingolipid clusters are the major component of these rafts and it has been shown that removal of cholesterol results in disturbances of signaling events normally taking place within these rafts (Keller and Simons, 1998; Moran and Miceli, 1998). The fact that preincubation of the cells in MCD drastically reduced vesicle formation suggests that c-kit is present in these rafts and that the integrity of functional rafts may be a prerequisite for internalization of c-kit following SCF stimulation.

Using our construct in combination with *in vivo* imaging we have been able to draw a detailed picture of the internalization process of c-kit following SCF induced activation.

Materials and methods

Reagents and antibodies

Mouse recombinant SCF was purchased from R&D Systems GmbH, Weisbaden, Germany. Polyclonal anti c-kit antibodies were obtained from Santa Cruz Biotechnology Inc., Heidelberg, Germany (C-19, rabbit, and M14, goat). Polyclonal anti-EGFP antibody was obtained from Clontech, Hamburg, Germany, the monoclonal antibody (12CA5) against the HA-Tag from Boehringer/Roche, Mannheim, Germany. Phospho-specific Akt antibody (Ser 473) from New England Biolabs GmbH (Schwalbach/Taunus, Germany). Anti-phosphotyrosine antibodies were purchased from Upstate Biotechnology, Lake Placid, NY, USA, (4G10) and Pharmingen, Hamburg, Germany (PY20). Primers were obtained from a commercial source (MWG-Biotech GmbH, Ebersberg, Germany). The HA tagged PKB/Akt construct was a generous gift from Dr Thomas Franke, Department of Pharmacology, Columbia University, New York, NY 10032, USA.

Cloning of c-kit-EGFP fusion constructs

All *c-kit* constructs used in this study were cloned into the mammalian expression vector pCDNA 3.1 (Invitrogen, Groningen, The Netherlands). *c-kit-EGFP*: The stop codon of the murine *c-kit* cDNA was deleted and a *Bam*HI site was inserted using PCR based primer extension. Using the same method a 3× glycine linker connected to a *Bam*HI site was added to the EGFP cDNA *SS-EYFP-kit*: Using PCR based site directed mutagenesis (Stratagene, Heidelberg, Germany) an *Eco*RI site was inserted directly downstream of the signal sequence of the murine *c-kit* cDNA using the following primer: 5′ CTG CTC CGT GGC CAG ACA GAA TTC GCC ACG TCT CAG CCA TCT GC 3′. The EYFP cDNA

was equipped with a linker of three glycines and flanking *Eco*RI sites and inserted into the mutated *c-kit* cDNA using the *Eco*RI site. The mutant *c-kit* constructs were obtained by PCR based site directed mutagenesis with primers containing the indicated amino acid changes on the nucleotide level. All mutations were verified by sequencing or restriction analysis, if possible.

Cell culture and transfection methods

293 and COS7 cells were maintained in DMEM (GIBCO–BRL, Karlsruhe, Germany) supplemented with 10% FCS (Biochrom KG, Berlin, Germany). 293 cells were transfected using DOTAP (Boehringer/Roche, Mannheim, Germany), COS7 cells were transfected using Gene Porter (GTS Inc., Biozol GmbH, Eching, Germany) according to the manufacturer's recommendations.

SCF stimulation

Cells were serum starved in DMEM lacking FCS for at least 6 h and stimulated with 500 ng/ml SCF for the times indicated.

Inhibition of c-kit internalization and proteasome inhibition

To inhibit c-kit internalization cells were incubated for 5 min with 50 μM PAO (phenylarsine oxide)/DMSO for 5 min at 37°C (Sigma, Taufkirchen, Germany). For proteasome inhibition cells were incubated for 5 min at 37°C in media containing lactacystin/MG132/Proteasome Inhibitor I/DMSO (Calbiochem-Novabiochem, Schwalbach, Germany) at a concentration of 10 μM. Control cells were incubated in media containing the same concentration of DMSO. Cells were rinsed twice with prewarmed DMEM lacking FCS before stimulation.

Disruption of lipid rafts

For cholesterol extraction with methyl-β-cyclodextrin (MCD) (Sigma, Taufkirchen, Germany) cells were incubated in DMEM containing MCD at the concentrations indicated for 45 min at 37°C. Control cells were incubated in media lacking MCD. Cells were washed twice with prewarmed media before stimulation with SCF.

Cell proliferation assay

3×10^4 cells per well were plated into 96-well plates in 200 μl of their respective media. After the indicated time period, the viable cells in each well were assayed for their ability to transform MTS (3-(4,5-dimethylthiazol-2-yl)-5-(3-carboxymethoxyphenyl)-2-(4-sulfophenyl)-2H-tetrazolium) (CellTiter 96®, Promega, Mannheim, Germany) into a purple formazan. Forty μl of a 10 mg/ml MTS solution were added in each well. After an incubation period of 4 h at 37°C the reaction was stopped by adding 50 μl 10% SDS and the absorbance of the samples was measured in an ELISA reader at 490 nm.

FACS analysis

Ba/F3 cells stably expressing c-kit WT were analysed for surface c-kit expression before and after 45′ treatment with 500 ng/ml SCF with or without addition of 75 μg/ml (267 μM) cycloheximide (Calbiochem, Darmstadt, Germany). Cells were analysed at 0, 45 and 90 min after the start of SCF stimulation. To assess reconstitution of c-kit at the cell surface, SCF containing media was removed, cells were washed three times with PBS and cultivated for the indicated additional time with or without cycloheximide. For detection of c-kit expression by FACS, cells were stained with a PE-labeled c-kit antibody (ACK45, Pharmingen, Heidelberg, Germany) or control antibody (A95-1, Pharmingen, Heidelberg, Germany) and measured on a Coulter XL FACS machine (Coulter, Krefeld, Germany) in the FL1 and FL2 gate.

Immunoprecipitations and immunoblotting

Immunoprecipitations and immunoblotting was done as previously described (Duyster *et al*., 1995). Briefly, SCF stimulated or non-stimulated cells were harvested in cold PBS containing 1 mM Sodium Vanadate, pelleted and lysed in lysis buffer containing 10 mM Tris-HCl (pH 7.4), 5 mM EDTA, 130 mM NaCl, 1% Triton, 1 mM phenylmethylsulfonyl fluoride, 1 mM Na_3VO_4 and 10 mg/ml of each phenantroline, aprotinin, leupeptin and pepstatin. After clarification by centrifugation and preclearing with protein A-Sepharose, antibody-protein complexes were brought down with 30 μl of protein A-Sepharose (Amersham/Pharmacia Biotech AB, Freiburg, Germany). For immunoprecipitation of *c-kit* 2 μg of anti-kit M14 was used. Lysates and bound fractions of immunoprecipitations were subjected to SDS–PAGE and blotting was performed on PVDF membranes (Immobilon-P, Millipore GmbH, Eschborn, Germany). Immunodetection of phosphotyrosine was done using a mixture of the anti-phosphotyrosine antibodies 4G10 and PY20. For detection of immunoprecipitated c-kit or c-kit from lysates anti-kit C19 was used. In order to examine activation of PKB/Akt lysates from cells overexpressing HA-tagged Akt were first analysed with an anti-phospho-Akt antibody. After stripping the same membrane was probed with an anti-HA antibody to verify equal expression levels of HA-Akt. Blots were developed using SuperSignal® chemoluminescent substrates from Pierce Chemical Company (KMF GmbH, St. Augustin, Germany).

Visualization of c-kit-EGFP fusion constructs in fixed cells

Fixation and detection of EGFP fusion constructs in fixed cells was done as previously described (Coutinho *et al*., 2000). Briefly, COS7 cells were cultured and transfected on gelatin-coated chamber slides (Nunc GmbH, Wiesbaden, Germany). Seventy-two hours after transfection, cells were starved for at least 6 h, stimulated with SCF as indicated, washed with cold PBS containing 1 mM Vanadate and fixed with 3.7% paraformaldehyde for 15 min. Cells were then washed twice with PBS, overlaid with mounting medium (Molecular Probes), covered with a coverslide and visualized using a fluorescence microscope (Olympus optical Co. GmbH, Hamburg, Germany) connected to a digital imaging system (TILL Photonics, Munich, Germany). For detection of different fluorochromes the appropriate filter sets were used (Chroma, AHF AG, Tuebingen, Germany). The fluorescence information of the c-kit-fusion constructs (green channel) was superimposed onto the transmission picture of the cell (red channel) in order to facilitate subcellular localization of the fluorescence signal.

Z-scan analysis

Manual Z-scan analysis was performed by focusing three levels (supranuclear: Red channel; epinuclear: Blue channel; peripheral: Green channel) of the adherent COS7 cell

showing vesicle formation after SCF stimulation. All three channels were digitally combined in the RGB picture.

Time lapse imaging of c-kit molecules in living cells

COS7 cells expressing SS-EYFP-kit were grown on a dish with an integrated coverslide. Using an inverted microscope (Olympus IX-50) equipped with a temperature control unit time lapse imaging of cells was performed at 37°C for 200 s with an imaging cycle time of 10 s. The sum of all vesicle movements during 200 s ($\Delta t = 200$ s) (red channel) was superimposed on the initial picture of the cell (green channel). The software for imaging vesicle tracks was kindly provided by TILL Photonics, Munich, Germany.

Acknowledgments
This work was supported by a grant to J Duyster from the José-Carreras Stiftung and Mildren-Scheel Siftung and by SFB grant No 456 to J Duyster and C Peschel. T Jahn and C Miething are supported by a fellowship from the Deutsche José-Carreras Stiftung. We thank Kenneth I Weinberg, Children's Hospital Los Angeles, for very helpful suggestions and comments and critically reading the manuscript. We thank Dr Christian Heinemann, TILL Photonics, for friendly and skilful support. We thank Claudia Mugler for technical assistance.

References

Beaumont V, Hepworth MB, Luty JS, Kelly E and Henderson G. (1998). *J. Biol. Chem.,* **273,** 33174–33183.
Beslu N, LaRose J, Casteran N, Birnbaum D, Lecocq E, Dubreuil P and Rottapel R. (1996). *J. Biol. Chem.,* **271,** 20075–20081.
Blume-Jensen P, Jiang G, Hyman R, Lee KF, O'Gorman S and Hunter T. (2000). *Nat. Genet.,* **24,** 157–162.
Broudy VC. (1997). *Blood,* **90,** 1345–1364.
Broudy VC, Lin NL, Buhring HJ, Komatsu N and Kavanagh TJ. (1998). *Blood,* **91,** 898–906.
Broudy VC, Lin NL, Liles WC, Corey SJ, O'Laughlin B, Mou S and Linnekin D. (1999). *Blood,* **94,** 1979–1986.
Carter RE and Sorkin A. (1998). *J. Biol. Chem.,* **273,** 35000–35007.
Caruana G, Cambareri AC and Ashman LK. (1999). *Oncogene,* **18,** 5573–5581.
Clarkson BD, Strife A, Wisniewski D, Lambek C and Carpino N. (1997). *Leukemia,* **11,** 1404–1428.
Coutinho S, Jahn T, Lewitzky M, Feller S, Hutzler P, Peschel C and Duyster J. (2000). *Blood,* **96,** 618–624.
De Angelis DA, Miesenbock G, Zemelman BV and Rothman JE. (1998). *Proc. Natl. Acad. Sci. USA,* **95,** 12312–12316.
Deberry C, Mou S and Linnekin D. (1997). *Biochem. J.,* **327,** 73–80.
Duyster J, Baskaran R and Wang JY. (1995). *Proc. Natl. Acad. Sci. USA,* **92,** 1555–1559.
Feng Y, Minnerly JC, Zurfluh LL, Joy WD, Hood WF, Abegg AL, Grabbe ES, Shieh JJ, Thurman TL, McKearn JP and McWherter CA. (1999). *Biochemistry,* **38,** 4553–4563.
Fischer M, Goldschmidt J, Peschel C, Brakenhoff JP, Kallen KJ, Wollmer A, Grotzinger J and Rose-John S. (1997). *Nat. Biotechnol.,* **15,** 142–145.
Gommerman JL, Rottapel R and Berger SA. (1997). *J. Biol. Chem.,* **272,** 30519–30525.
Gordon GW, Berry G, Liang XH, Levine B and Herman B. (1998). *Biophys J.,* **74,** 2702–2713.
Hallek M, Danhauser-Riedl S, Herbst R, Warmuth M, Winkler A, Kolb HJ, Druker B, Griffin JD, Emmerich B and Ullrich A. (1996). *Br. J. Haematol.,* **94,** 5–16.
Joly M, Kazlauskas A and Corvera S. (1995). *J. Biol. Chem.,* **270,** 13225–13230.
Kanakura Y, Furitsu T, Tsujimura T, Butterfield JH, Ashman LK, Ikeda H, Kitayama H, Kanayama Y, Matsuzawa Y and Kitamura Y. (1994). *Leukemia,* **8** (Suppl 1), S18–S22.
Keller P and Simons K. (1998). *J. Cell. Biol.,* **140,** 1357–1367.
Krystal GW, DeBerry CS, Linnekin D and Litz J. (1998). *Cancer Res.,* **58,** 4660–4666.
Kurzchalia TV and Parton RG. (1999). *Curr. Opin. Cell. Biol.,* **11,** 424–431.
Langley KE, Bennett LG, Wypych J, Yancik SA, Liu XD, Westcott KR, Chang DG, Smith KA and Zsebo KM. (1993). *Blood,* **81,** 656–660.
Lennartson J, Blume-Jensen P, Hermanson M, Ponten E, Carlberg M and Ronnstrand L. (1999). *Oncogene,* **18,** 5546–5553.
Li Q, Kondoh G, Inafuku S, Nishimune Y and Hakura A. (1996). *Cancer Res.,* **56,** 4343–4346.
Liu L, Cutler RL, Mui AL and Krystal G. (1994). *J. Biol. Chem.,* **269,** 16774–16779.
Longley BJ, Tyrrell L, Ma Y, Williams DA, Halaban R, Langley K, Lu HS and Schechter NM. (1997). *Proc. Natl. Acad. Sci. USA,* **94,** 9017–9021.
Mahajan NP, Linder K, Berry G, Gordon GW, Heim R and Herman B. (1998). *Nat. Biotechnol.,* **16,** 547–552.
Miyazawa K, Toyama K, Gotoh A, Hendrie PC, Mantel C and Broxmeyer HE. (1994). *Blood,* **83,** 137–145.
Moran M and Miceli MC. (1998). *Immunity,* **9,** 787–796.
Oliferenko S, Paiha K, Harder T, Gerke V, Schwarzler C, Schwarz H, Beug H, Gunthert U and Huber LA. (1999). *J. Cell. Biol.,* **146,** 843–854.
Serve H, Yee NS, Stella G, Sepp-Lorenzino L, Tan JC and Besmer P. (1995). *EMBO J.,* **14,** 473–483.
Shimizu Y, Ashman LK, Du Z and Schwartz LB. (1996). *J. Immunol.,* **156,** 3443–3449.
Simons K and Ikonen E. (1997). *Nature,* **387,** 569–572.
Thommes K, Lennartsson J, Carlberg M and Ronnstrand L. (1999). *Biochem. J.,* **341,** 211–216.
Timokhina I, Kissel H, Stella G and Besmer P. (1998). *EMBO J.,* **17,** 6250–6262.
Wakioka T, Sasaki A, Mitsui K, Yokouchi M, Inoue A, Komiya S and Yoshimura A. (1999). *Leukemia,* **13,** 760–767.
Wu H, Klingmuller U, Besmer P and Lodish HF. (1995). *Nature,* **377,** 242–246.
Yee NS, Hsiau CW, Serve H, Vosseller K and Besmer P. (1994). *J. Biol. Chem.,* **269,** 31991–31998.